University of Dundee

Original Reaction Sequence of Pb(Yb1/2Nb1/2)O3-PbTiO3

Cochard, Charlotte; Karolak, Fabienne; Bogicevic, Christine; Guedes, Orland; Janolin, Pierre-Eymeric

Citation for published version (APA):
Cochard, C., Karolak, F., Bogicevic, C., Guedes, O., & Janolin, P-E. (2015). Original Reaction Sequence of Pb(Yb$_{1/2}$Nb$_{1/2}$)O$_3$-PbTiO$_3$: Consequences on dielectric properties and chemical order. *Advances in Materials Science and Engineering*, *2015*, [408101]. https://doi.org/10.1155/2015/408101

Research Article

Original Reaction Sequence of $Pb(Yb_{1/2}Nb_{1/2})O_3$-$PbTiO_3$: Consequences on Dielectric Properties and Chemical Order

Charlotte Cochard,[1,2] Fabienne Karolak,[1] Christine Bogicevic,[1] Orland Guedes,[2] and Pierre-Eymeric Janolin[1]

[1]*Laboratoire SPMS, Université Paris Saclay, CentraleSupélec, CNRS; Grande Voie des Vignes, 92295 Chatenay-Malabry, France*
[2]*Études et Productions Schlumberger, 1 rue Henri Becquerel, 92140 Clamart, France*

Correspondence should be addressed to Pierre-Eymeric Janolin; pierre-eymeric.janolin@centralesupelec.fr

The solid solution $[Pb(Yb_{1/2}Nb_{1/2})O_3]_{1-x}$-$[PbTiO_3]_x$ was synthesized with $x \leq 60\%$, using several high-temperature techniques as well as room-temperature mechanosynthesis. The high-temperature synthesis reveals a reaction path involving the synthesis first of the end-members before the solid solution. The density and dielectric constant measured on the ceramics prepared from these powders indicate the crucial role of the synthesis technique in the subsequent properties. Mechanosynthesis results in ceramics with higher density and dielectric constant. Identical optimized sintering conditions were then applied to all investigated compositions and the resulting dielectric properties and chemical orders were compared. All polar orders (antiferroelectricity, ferroelectricity, and relaxor behavior) were evidenced. The 1 : 1 chemical order on the B-site of $Pb(Yb_{1/2}Nb_{1/2})O_3$ results in the formation of a double perovskite Pb_2YbNbO_6, and the superstructures in the X-ray diagrams signing the existence of this order persist up to 30% $PbTiO_3$. The underlying mechanism for substitution of Yb or Nb by Ti is presented.

1. Introduction

Solid solution between ferroelectric $PbTiO_3$ and perovskites with two elements on the B site (of the general formula $A(BB')O_3$) have attracted considerable interest as they lead to high-performance functional materials such as $Pb(Mg_{1/3},Nb_{2/3})O_3$-$PbTiO_3$ [1], $Pb(Zn_{1/3},Nb_{2/3})O_3$-$PbTiO_3$ [2], $Pb(Sc_{1/2},Nb_{1/2})O_3$-$PbTiO_3$ [3], and $Pb(In_{1/2},Nb_{1/2})O_3$-$PbTiO_3$ [4], which are of both fundamental and commercial interests. $Pb(Yb_{1/2}Nb_{1/2})O_3$-$PbTiO_3$ is one of such materials. It exhibits superior high-temperature high-piezoelectric properties, especially at the so-called "morphotropic" phase boundary with a Curie temperature of 370°C (645 K) and a piezoelectric coefficient $d_{33} \sim 470$–510 pC/N [5, 6] which makes it desirable for high-temperature actuators and sensors.

The synthesis of these $A(BB')O_3$ compounds is delicate as pyrochlore phases may easily be formed when all oxides are reacting and are detrimental to the properties. An alternative synthesis route has been designed for $Pb(BB')O_3$ perovskites, the so-called "B-site oxide mixing route" [7, 8] involving the reaction of all oxides but PbO. Depending on the valence of the B-site elements, this leads to the synthesis of a columbite through $B^{2+}O^{2-} + B'^{5+}_2O^{2-}_5 \rightarrow BB'_2O_6$ [9] or of a wolframite through $B^{3+}_2O^{2-}_3 + B'^{5+}_2O^{2-}_5 \rightarrow 2BB'O_4$ [10] or of a rutile through $B^{4+}O^{2-}_2 + B'^{4+}O^{2-}_2 \rightarrow BB'O_4$ [11]. In a second step, this columbite, wolframite, or rutile is mixed with PbO to get $Pb(B,B')O_3$. For $Pb(B,B')O_3$-$PbTiO_3$ solid solution, either TiO_2 is added to the other B-site oxides and then PbO is added to the product of this reaction [7, 8] or TiO_2 + PbO is added to the wolframite/columbite/rutile [1–4].

In the case of $Pb(B_{1/2}B'_{1/2})O_3$ ferroelectric perovskites, the order on the B site has a dramatic influence on the properties of these materials. Generally speaking, disorder on the B site of the perovskite (i.e., random occupancy by any of the two elements) leads to a relaxor behavior whereas an ordered alternating occupancy of the B site along the [111]

direction by the two elements leads generally to antiferro-electric behavior [12, 13]. In the latter case, the structure may be described as a "double perovskite" of general formula $Pb_2BB'O_6$. This order doubles the crystallographic unit cell along the [111] direction, giving rise to superstructure X-ray reflections, and was shown to be driven more by the sum of the ionization energies of the two B-site elements rather than by size or charge difference [14]. In the case of $Pb(Yb_{1/2}Nb_{1/2})O_3$ (PYN), the sum of the ionization energies is large (75 eV) leading to a 1:1 chemical order on the B site which could only be broken by adding lithium to the compound [15].

In this work we investigate three techniques to synthesize $[Pb(Yb_{1/2}Nb_{1/2})O_3]_{1-x}$-$[PbTiO_3]_x$ (PYN-PT) with $x \leq$ 60% (Ti-richer compositions were considered analogous to $PbTiO_3$) and compared the properties of the ceramics made out of these powders. The investigated techniques are conventional solid-state mixing, reactive sintering, and mechanosynthesis. An original intermediate reaction step involving the formation of the two end-members is evidenced. The chemical order on the B-site, reminiscent of the one of PYN, is shown to persist in the powders obtained from mechanosynthesis up to composition with 30% $PbTiO_3$.

2. Experimental Procedure

Commercial-grade oxides PbO (Interchim), Yb_2O_3 (Rhône-Poulenc), Nb_2O_5, and TiO_2 (both Alfa Aesar) with purity greater than 99.5% were used as starting materials. Raw materials were mixed in absolute ethanol and subsequently dried in a dry-off oven at 80°C for 24 h before calcination. For every synthesis technique used, the first step consisted in obtaining the $YbNbO_4$ wolframite from the calcination of Yb_2O_3 and Nb_2O_5 at 1200°C for 4 h. For the synthesis of the solid solution, and still for every synthesis techniques, we followed the conventional route, mixing stoichiometric quantities of PbO, TiO_2, and $YbNbO_4$.

For the solid-state technique, we investigated various calcination temperatures and times (800–1000°C and 2–12 h) to get the pure perovskite phase. The reactive sintering technique, as its name indicates, enables carrying out both the synthesis and the sintering of the ceramics from a pellet composed of the reactants [11]. For all compositions investigated, the optimized conditions for simultaneous synthesis and sintering were 950 to 1050°C for 4 h. For the mechanosynthesis, we used a Retsch mill PM 100, and the pure perovskite phase was obtained after 9 h at 450 rpm. This process takes place at room temperature as the thermal energy of the other techniques is replaced here by mechanical energy.

The X-ray diffraction was carried out on a Bruker D2 phaser to check the crystallinity and purity of the products and on an 18 kW high-precision diffractometer equipped with a rotating Cu anode for the superstructures detection. The X-ray diagrams were either compared with the corresponding JCPDS file (for $PbTiO_3$) or to the literature [16] (for $Pb(Yb_{1/2}Nb_{1/2})O_3$, as no JCPDS file is available) to confirm the perovskite phase and its purity. Scanning Electronic Microscopy (SEM) and Energy Dispersive X-ray Spectroscopy (EDX) (Leo Gemini 5130) were performed on
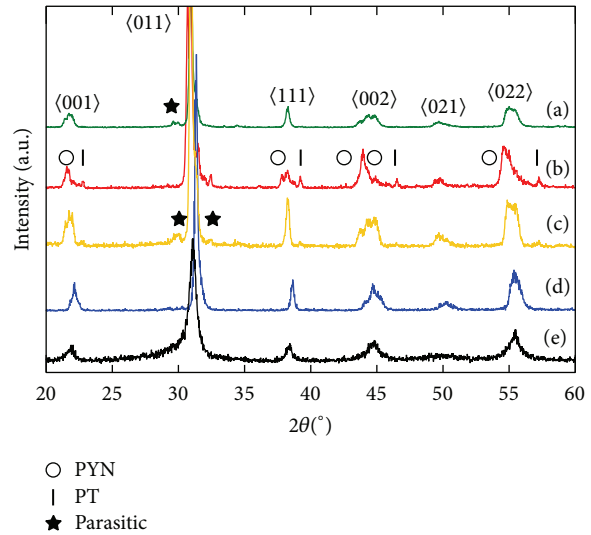

FIGURE 1: X-ray diagram of PYN-PT powder (for $x = 60\%$) obtained by various techniques: at 950°C by solid-state reaction of PbO + TiO_2 + $YbNbO_4$ (a) for 7 h and (b) for shorter calcination time (4 h) revealing the presence of PYN and PT and (c) by solid-state reaction of $Pb(Yb_{1/2}Nb_{1/2})O_3$ + $PbTiO_3$ leading to PYN-PT after 4 h. Pure PYN-PT can be synthesized by solid-state reaction at 800°C for 12 h (d) as well as by mechanosynthesis (e) of PbO + TiO_2 + $YbNbO_4$.

fractured surfaces to investigate the purity and microstructure of the samples. The average grain sizes were determined using the line interception method on SEM images [17]. The relative density was calculated using geometrical dimension or the Archimedes' method. Dielectric measurements were carried out using an Agilent 4294A impedance analyzer on ceramics with gold-sputtered electrodes.

3. Results and Discussion

Starting with the conventional solid-state technique, after 7 h at 950°C, PYN-PT is formed (see Figure 1(a)). However, for shorter calcination times (4 h), extra diffraction peaks related to $Pb(Yb_{1/2}Nb_{1/2})O_3$ and $PbTiO_3$ also appear in Figure 1(b). This suggests that the reaction sequence is actually PbO + TiO_2 + $YbNbO_4$ → $Pb(Yb_{1/2}Nb_{1/2})O_3$ + $PbTiO_3$ → PYN-PT. It is highly unusual that the reaction sequence of such a solid solution involves forming first the end-members. In order to test whether it is actually possible to synthesize the solid solution from its end-members, we synthesized $Pb(Yb_{1/2}Nb_{1/2})O_3$ and $PbTiO_3$ separately, before mixing them and calcining them for 950°C 4 h. We indeed obtained PYN-PT, as can be seen in Figure 1(c). The pyrochlore impurity phase can be eliminated and pure PYN-PT synthesized under optimized synthesis conditions (namely, at 800°C for 12 h); see Figure 1(d).

Pyrochlore phases have been shown to form at moderate temperatures (600–700°C) in $Pb(BB')O_3$ and $Pb(BB')O_3$-$PbTiO_3$ solid solutions, even using the B-site mixing route [7, 9, 18, 19], and may still be present in the final product. In PYN-PT, a pyrochlore phase may also be formed but then the end-members, PYN and PT, are formed before reacting together

to form the PYN-PT solid solution at higher temperature. With optimized synthesis parameters it is possible to obtain pyrochlore-free PYN-PT samples.

The powder of pure perovskite obtained from solid-state synthesis must be shaped and sintered in order to get the final ceramic. As the reaction temperature and the sintering temperature were the same, a more practical solution to prepare ceramics was investigated: reactive sintering. In this case, the raw reactants are prepressed into a so-called "green" pellet and both the calcination and sintering occur simultaneously. Following this route we observed the same reaction sequence that starting from PbO + YbNbO$_4$ + TiO$_2$ leads to the formation of PYN and PbTiO$_3$ and only afterwards of PYN-PT.

In order to prevent the formation of pyrochlore phases, alternative high-pressure and/or high-temperature techniques have been developed, for example, hot isostatic press. They, however, require heavy equipment. The last technique used to synthesize PYN-PT, mechanosynthesis, was shown to enable the synthesis of pure perovskite phase without such heavy equipment. This room-temperature technique, also known as ball-milling, was first applied to metallic alloys in the late 70s and to ferroelectric oxides 20 years later [8, 20, 21]. The strain and the grain size reduction taking place during the mechanosynthesis lead to broad and asymmetric peaks in the diffraction patterns making the identification of minority phases in presence difficult. The pure perovskite phase was considered to be obtained when subsequent milling did not change the diffraction pattern. The corresponding X-ray diagram is reported in Figure 1(e) where the large width and asymmetric profile of the peaks associated with the mechanical strain developed in the nanograins can be clearly observed. The difference with the high-temperature synthesis techniques here is that the grain size of the reactants is much smaller (~20 nm versus microsized grains) and therefore present a much higher reactivity.

Powders obtained by the solid-state or mechanosynthesis techniques have been sintered (at 950°C for 4 h) and the absence of pyrochlore after sintering was confirmed by X-ray diffraction (not shown). The density and dielectric constant at room temperature of the resulting ceramics are compared with the ceramics obtained by reactive sintering in Table 1. The dielectric constants reported in Table 1 have been normalized by the density of the ceramic to enable a meaningful comparison. Because the ceramics prepared from reactive sintering have an extremely low density and therefore open pores, their dielectric constants value cannot be simply compared to the ones of ceramics prepared by the other processing methods. However, it clearly appears that processing ceramics by reactive sintering leads to ceramics of poor quality that are unsuitable for potential applications. The ceramics obtained from mechanosynthesis are the densest and exhibit the highest dielectric constant of all investigated synthesis techniques. A binder was necessary to shape the powder obtained by the solid-state technique into pellets before sintering. In the case of the first binder used, PVA, SEM, and EDX analyses confirmed the absence of carbonated residues after sintering. Addition of PbO instead of PVA was also considered as high-temperature synthesis may lead to

Table 1: Relative density (d) and normalized dielectric constant (ϵ'/d) at room temperature and 1 kHz measured on PYN-PT ceramics with 60% PbTiO$_3$ obtained by the various investigated synthesis techniques. For the solid-state technique, PVA or PbO were used as binders.

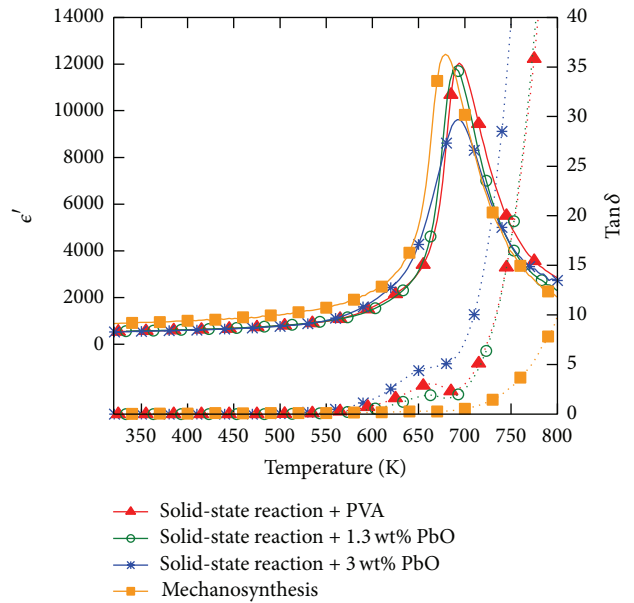|	d	ϵ'/d
Reactive sintering	60%	302
Solid-state reaction + PVA	81%	652
Solid-state reaction + 1.3 wt% PbO	72%	771
Solid-state reaction + 3 wt% PbO	86%	613
Mechanosynthesis	91%	953

Figure 2: Real part of the dielectric constant ϵ' (line) and losses tan δ (dotted line) of PYN-PT with 60% PbTiO$_3$ measured at 1 kHz and as a function of temperature on ceramics obtained by various synthesis techniques: +PVA, +1 wt% PbO, and +3 wt% PbO designate the binder used with powders obtained by the solid-state technique. All samples were sintered at 950°C.

Pb evaporation. PbO may also act as a liquid sintering aid. The results are contrasted: if the ceramics density increases with PbO excess compared to reactive sintering, adding 3 wt% excess PbO leads to a normalized dielectric constant lower than with a 1.3 wt% excess PbO. This is because the excess PbO overcompensates for Pb loss during sintering and remains as PbO in the ceramics. Its low dielectric constant (~20) therefore contributes to lowering the ceramic dielectric constant.

The influence of the synthesis technique on dielectric properties is presented in Figure 2. Mechanosynthesis leads to the highest dielectric constant at the para-ferroelectric phase transition ($T_C \sim 530$°C) with $\epsilon'_{max} > 12\,000$. The ceramics obtained from solid-state technique exhibit slightly lower ϵ'_{max}, and, as mentioned earlier, excess of PbO decreases ϵ'_{max}. From SEM, we found that, even after sintering, the grain size of PYN-PT obtained by mechanosynthesis remains smaller (~1 μm) than with other techniques (≥ 5 μm).
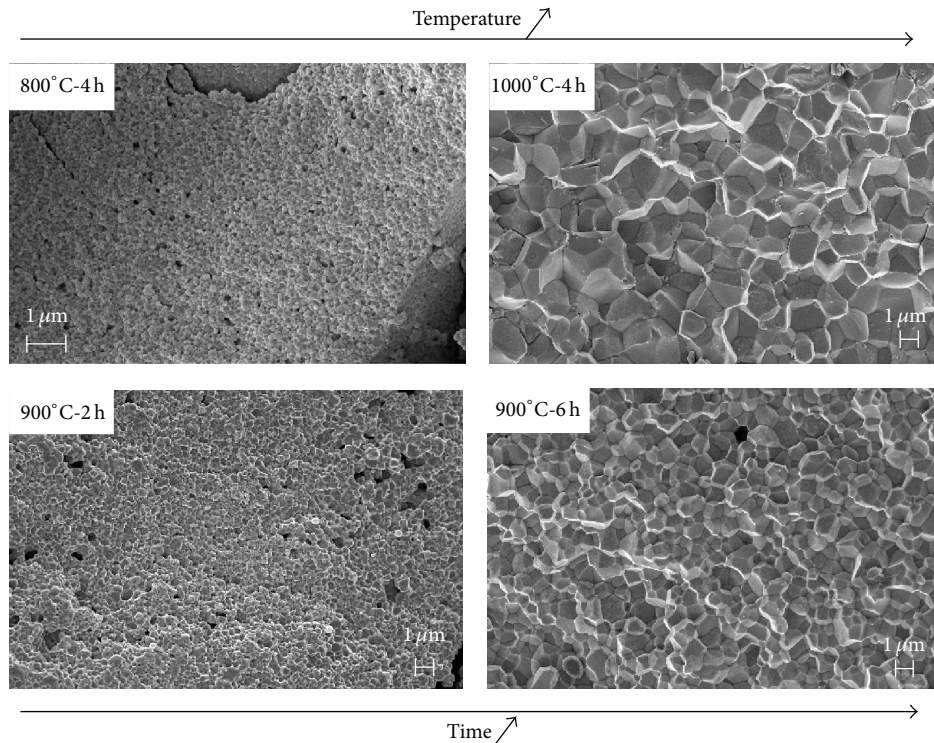
FIGURE 3: SEM images of PYN-PT 60% ceramics obtained after sintering at various temperatures and times.

The grain size of ceramics obtained from mechanosynthesis is close to the optimum grain size of Pb-based perovskites giving rise to the best properties. This smaller grain size, combined with strain effects [22], also contributes to lowering the transition temperature by ~10°C.

Sintering conditions for ceramics obtained by mechanosynthesis were then further optimized with the objective to determine sintering parameters valid over the entire compositional range investigated here (from 0 to 60% PbTiO$_3$). The SEM investigation reveals that, as expected, the grain size increases with increasing sintering temperature and time. Taking the example of PYN-PT 0.60 (Figure 3), the grain size increases from 0.086 μm to 1.27 μm when increasing the sintering temperature from 800 to 1000°C and keeping the sintering time constant at 4 h. A similar increase is observed when increasing the sintering time (from 0.25 μm at 900°C for 2 h to 0.78 μm at 900°C for 6 h). Together with the decrease in the number and size of porosities, this larger grain size leads to an increase of the dielectric constant [1, 4] (Figure 4). At the smallest grain size (0.086 μm), the dielectric peak at the Curie temperature is broad but still existent indicating the persistence of the ferroelectric properties down to this grain size. Comparable increase of grain size with sintering temperature/time was observed for other compositions within the PYN-PT solid solution.

The evolution of the dielectric constant with temperature and the room-temperature diffractograms for selected compositions is presented in Figures 5 and 6, in order to show that antiferroelectric (pure PYN [23, 24] and PYN-5% PT
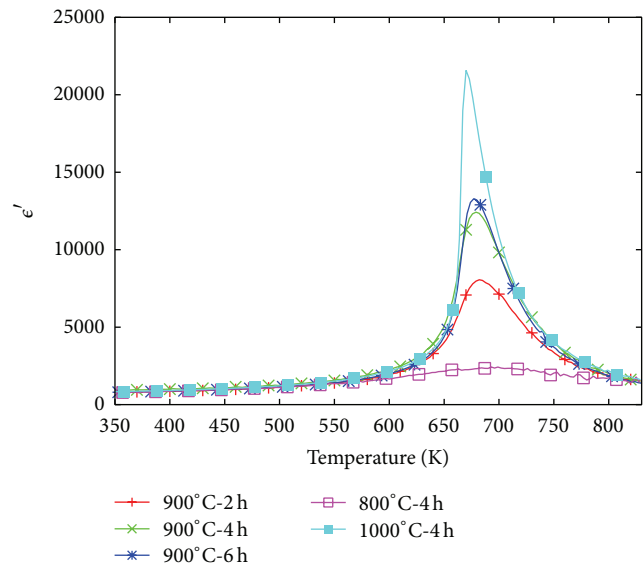

FIGURE 4: Real part of the dielectric constant (ϵ') measured at 1 kHz from RT to 530°C of PYN-PT 60% ceramic obtained from various sintering temperatures and times.

[25, 26]), relaxor (for 25, 30, and 40% PbTiO$_3$ content) and ferroelectric compositions (50 and 60% PbTiO$_3$ content) can be synthesized by this method. Our study focuses on the synthesis of the ceramics, and the complete description of
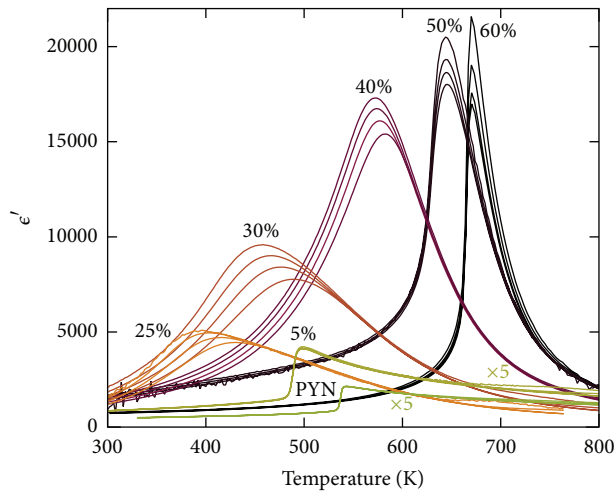
FIGURE 5: Real part of the dielectric constant (ϵ') measured at 1 kHz from RT to 530°C on PYN-PT ceramics exhibiting antiferroelectric (pure PYN and PYN-5% PT), relaxor (for 25, 30, and 40% $PbTiO_3$ content), or ferroelectric (50 and 60% $PbTiO_3$ content) behaviors. All samples were sintered between 950°C and 1050°C.
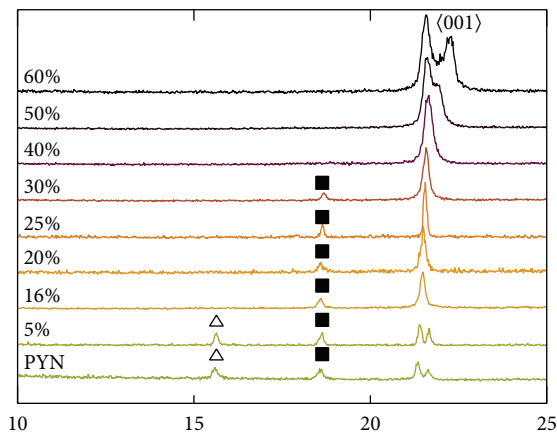

FIGURE 6: X-ray diagrams for PYN-PT ceramics obtained by mechanosynthesis for $PbTiO_3$ content between 0 (PYN) and 60%. Squares (■) indicate superstructure reflections due to chemical order on the B site. Triangles (△) mark superstructures due to antiparallel displacements. All samples were sintered between 950°C and 1050°C.

their properties together with the type of ferroelectric order they derivate from shall be presented elsewhere.

Figure 6 exhibits superstructure reflections (marked with a square) indicating that the chemical B-site order of PYN persists for PYN-PT compositions with $PbTiO_3$ content up to 30% with no indication of Ti segregation (broadening of reflections, lowering of intensity, etc.). This chemical order reflects an equally probable substitution of Ytterbium and Niobium by Titanium. The details of the microstructural model explaining the origin of these superstructures will be published elsewhere but let us give nevertheless the main

idea here. It stems from the strong stability of the Yb/Nb order on the B site of PYN which has been evidenced as an intermediate step in the solid-state synthesis technique. Starting from pure PYN, we mentioned before that the chemical formula of this double perovskite may be written Pb_2YbNbO_6 in order to reflect the chemical order existing on the B site along the [111] crystallographic direction. When $PbTiO_3$ is added, Titanium atoms substitute equally each B site (i.e., Yb or Nb), in order to preserve electroneutrality. This is coherent with the intermediate reaction step observed with high-temperature techniques where the end-members are formed before the solid solution. In this scheme, Titanium disturbs a preexisting order rather than inserting itself in-between Yb/Nb chains; that is, along the [111] direction, the alternation of B-cations would be $[Yb-Nb]_n$-Ti-$[Yb-Nb]_n$-Ti. This situation can be safely rejected since it would lead to a new chemical order and the superstructure reflections would be significantly shifted in the X-ray diagram with respect to their position in PYN. The composition $[Pb(Yb_{1/2}Nb_{1/2})O_3]_{1-x}$-$[PbTiO_3]_x$ may then be written $Pb_2(Yb_{1-x}Ti_x)(Nb_{1-x}Ti_x)O_6$ to reflect the underlying 1:1 chemical order giving rise to the superstructures reported in Figure 6. It is only when there are, on average, more Titanium atoms on the B sites than Ytterbium or Niobium atoms (i.e., for compositions with $PbTiO_3$ content over 33%) that the chemical order is broken and the corresponding superstructures disappear from the X-ray diagram. Such disordered compositions (with Ti content larger than 33%) may be then written $Pb(Yb_{1-x/2},Nb_{1-x/2},Ti_x)O_3$ and the structure of PYN-PT solid solution is described as a simple perovskite.

4. Conclusion

In conclusion we have shown that the end-members of the solid solution $Pb(Yb_{1/2}Nb_{1/2})O_3$-$PbTiO_3$ are formed first before the solid solution is obtained in high-temperature synthesis techniques, using the B-site oxides mixing route. Mechanosynthesis was shown to provide a room-temperature alternative to these techniques leading to ceramics with smaller grains but higher dielectric properties and density. Sintering conditions were optimized for all powders with $PbTiO_3$ content up to 60% and lead to ceramics exhibiting the full diversity of ferroelectric behaviors. From a structural point of view, the so-obtained ceramics exhibit a signature of B-site order reminiscent of the PYN one for compositions up to 30%, that is up to when there is an equal number of Titanium, Ytterbium, and Niobium on the B site of the perovskite.

Conflict of Interests

The authors declare that there is no conflict of interests regarding the publication of this paper.

Acknowledgment

References

[1] J. Carreaud, P. Gemeiner, J. M. Kiat et al., "Size-driven relaxation and polar states in PbMg$_{1/3}$Nb$_{2/3}$O$_3$-based system," *Physical Review B—Condensed Matter and Materials Physics*, vol. 72, no. 17, Article ID 174115, pp. 4–9, 2005.

[2] M. A. Hentati, H. Dammak, H. Khemakhem, and M. P. Thi, "Dielectric properties and phase transitions of [001], [110], and [111] oriented Pb(Zn$_{1/3}$Nb$_{2/3}$)O$_3$-6%PbTiO$_3$ single crystals," *Journal of Applied Physics*, vol. 113, no. 24, Article ID 244104, 2013.

[3] R. Haumont, B. Dkhil, J. M. Kiat, A. Al-Barakaty, H. Dammak, and L. Bellaiche, "Cationic-competition-induced monoclinic phase in high piezoelectric (PbSc$_{1/2}$Nb$_{1/2}$O$_3$)$_{1-x}$–(PbTiO$_3$)$_x$ compounds," *Physical Review B*, vol. 68, no. 1, Article ID 014114, 2003.

[4] K. Alilat, M. P. Thi, H. Dammak, C. Bogicevic, A. Albareda, and M. Doisy, "Grain size effect on electromechanical properties and non-linear response of dense nano and microstructured PIN-PT ceramics," *Journal of the European Ceramic Society*, vol. 30, no. 9, pp. 1919–1924, 2010.

[5] J. B. Lim, S. Zhang, and T. R. Shrout, "Relaxor behavior of piezoelectric Pb(Yb$_{1/2}$Nb$_{1/2}$)O$_3$-PbTiO$_3$ ceramics sintered at low temperature," *Journal of Electroceramics*, vol. 26, no. 1–4, pp. 68–73, 2011.

[6] T. Yamamoto and S. Ohashi, "Dielectric and piezoelectric properties of Pb(Yb$_{1/2}$Nb$_{1/2}$)O$_3$-PbTiO$_3$ solid solution system," *Japanese Journal of Applied Physics*, vol. 34, no. 9, pp. 5349–5353, 1995.

[7] M. Orita, H. Satoh, K. Aizawa, and K. Ametani, "Preparation of ferroelectric relaxor Pb(Zn$_{1/2}$Nb$_{2/3}$)O$_3$-Pb(Mg$_{1/3}$Nb$_{2/3}$)O$_3$-PbTiO$_3$ by two-step calcination method," *Japanese Journal of Applied Physics*, vol. 31, no. 9, part 1, pp. 3261–3264, 1992.

[8] R. M. V. Rao, A. Halliyal, and A. M. Umarji, "Perovskite phase formation in the relaxor system [Pb(Fe$_{1/2}$Nb$_{1/2}$)O$_3$]$_{1-x}$-[Pb(Zn$_{1/3}$Nb$_{2/3}$)O$_3$]$_x$," *Journal of the American Ceramic Society*, vol. 79, no. 1, pp. 257–260, 1996.

[9] S. L. Swartz and T. R. Shrout, "Fabrication of perovskite lead magnesium niobate," *Materials Research Bulletin*, vol. 17, no. 10, pp. 1245–1250, 1982.

[10] P. Groves, "Fabrication and characterisation of ferroelectric perovskite lead indium niobate," *Ferroelectrics*, vol. 65, no. 1, pp. 67–77, 2011.

[11] T. R. Shrout, P. Papet, S. Kim, and G.-S. Lee, "Conventionally prepared submicrometer lead-based perovskite powders by reactive calcination," *Journal of the American Ceramic Society*, vol. 73, no. 7, pp. 1862–1867, 1990.

[12] C. Cochard, *Pb(Yb$_{1/2}$Nb$_{1/2}$)O$_3$-PbTiO$_3$: a model solid solution for the study of polar orders [Ph.D. thesis]*, École Centrale Paris, Châtenay-Malabry, France, 2015.

[13] V. A. Isupov, "Ferroelectric and antiferroelectric perovskites PbB′0.5B″0.5O3," *Ferroelectrics*, vol. 289, no. 1, pp. 131–195, 2003.

[14] A. A. Bokov, N. P. Protsenko, and Z.-G. Ye, "Relationship between ionicity, ionic radii and order/disorder in complex perovskites," *Journal of Physics and Chemistry of Solids*, vol. 61, no. 9, pp. 1519–1527, 2000.

[15] A. A. Bokov, V. Y. Shonov, I. P. Rayevsky, E. S. Gagarina, and M. F. Kupriyanov, "Compositional ordering and phase transitions in Pb(Yb$_{0.5}$Nb$_{0.5}$)O$_3$," *Journal of Physics: Condensed Matter*, vol. 5, no. 31, pp. 5491–5504, 1993.

[16] W. K. Choo, H. J. Kim, J. H. Yang et al., "Crystal structure and B-site ordering in antiferroelectric Pb(Mg$_{1/2}$W$_{1/2}$)O$_3$, Pb(Co$_{1/2}$W$_{1/2}$)O$_3$ and Pb(Yb$_{1/2}$Nb$_{1/2}$)O$_3$," *Japanese Journal of Applied Physics*, vol. 32, no. 9, pp. 4249–4253, 1993.

[17] American Society for Testing and Materials, "Standard test methods for determining average grain size," ASTM E112-13, ASTM International, West Conshohocken, Pa, USA, 2013.

[18] V. V. Bhat, M. V. Radhika Rao, and A. M. Umarji, "Dilatometric approach for the determination of the solid state reaction-onset of the lead based relaxor ferroelectric system," *Materials Research Bulletin*, vol. 38, no. 6, pp. 1081–1090, 2003.

[19] Y. Zupei, Z. Shaorong, Q. Shaobo, C. Bin, and T. Changsheng, "Reaction mechanisms of PMN-PT powder prepared by molten salt synthesis," *Ferroelectrics*, vol. 265, no. 1, pp. 225–232, 2002.

[20] J. Xue, D. Wan, S.-E. Lee, and J. Wang, "Mechanochemical synthesis of lead zirconate titanate from mixed oxides," *Journal of the American Ceramic Society*, vol. 82, no. 7, pp. 1687–1692, 1999.

[21] J. Xue, J. Wang, and D. Wan, "Nanosized barium titanate powder by mechanical activation," *Journal of the American Ceramic Society*, vol. 83, no. 1, pp. 232–234, 2000.

[22] M. Algueró, J. Ricote, T. Hungría, and A. Castro, "High-sensitivity piezoelectric, low-tolerance-factor perovskites by mechanosynthesis," *Chemistry of Materials*, vol. 19, no. 20, pp. 4982–4990, 2007.

[23] V. Demidova, E. Gagarina, T. Ivanova, and V. Sakhnenko, "Atomic structure and phase transitions in antiferroelectric PbYb$_{0.5}$Nb$_{0.5}$O$_3$," *Ferroelectrics*, vol. 159, pp. 191–196, 1994.

[24] J. R. Kwon and W. K. Choo, "The antiferroelectric crystal structure of the highly ordered complex perovskite Pb(Yb$_{1/2}$Nb$_{1/2}$)O$_3$," *Journal of Physics: Condensed Matter*, vol. 3, no. 13, pp. 2147–2155, 1991.

[25] S.-J. Ahn, J.-J. Kim, J.-H. Kim, and W.-K. Choo, "Nondegenerate hard-mode Raman studies of phase transition in antiferroelectric lead ytterbium niobate-based perovskite compound," *Journal of Raman Spectroscopy*, vol. 37, no. 1–3, pp. 202–207, 2006.

[26] H. Lim, H. J. Kim, and W. K. Choo, "X-ray and dielectric studies of the phase transitions in Pb(Yb$_{1/2}$Nb$_{1/2}$)O$_3$-PbTiO$_3$ ceramics," *Japanese Journal of Applied Physics B*, vol. 34, no. 9, pp. 5449–5452, 1995.